Supporting Information

Porous PdRh Nanobowls: Facile Synthesis and Active for Alkaline Ethanol Oxidation

Zhijuan Li,[a, #] *Yifan Chen,*[a, #] *Gengtao Fu,*[b,*] *Yang Chen,* [a] *Dongmei Sun,* [a] *Jong-Min Lee*[b,*] *and Yawen Tang*[a,*]

[a]Jiangsu Key Laboratory of New Power Batteries, Jiangsu Collaborative Innovation Center of Biomedical Functional Materials, School of Chemistry and Materials Science, Nanjing Normal University, Nanjing 210023, China.

[b] School of Chemical and Biomedical Engineering, Maritime Institute, Nanyang Technological University, Singapore 637459, Singapore.

Part I: Materials and Methods

Reagents and Chemicals

Potassium palladium chloride (K_2PdCl_4), Rhodium Chloride Hydrate ($RhCl_3 \cdot 3H_2O$), urea, polyvinylpyrrolidone (PVP, Mw = 30 000) and ethanol (CH_3CH_2OH) were purchased from Sinopharm Chemical Reagent Co., Ltd. (Shanghai, China). Commercial Pd black was purchased from Johnson Matthey Corporation. All reagents were of analytical reagent grade and used without further purification.

Synthesis

Typically, 1.5 mL of 0.05 M K_2PdCl_4 solution, 0.5 mL of 0.05 M $RhCl_3 \cdot 3H_2O$ solution and 1.0 mL of 0.1 M urea were added into 7.0 ml deionized water with continuous ultrasonic for 30 minutes at room temperature. Then, 50 mg PVP polymer was added into above mixture solution with another continuous ultrasonic for 30 minutes. After adjusting solution pH to 12.0 using NaOH solution, the solution was transferred to a 20 mL Teflon-lined stainless-steel autoclave. The stainless-steel autoclave was heated at 140 °C for 4 h. After cooling to room temperature, the products were separated by centrifugation at 15000 rpm for 5 min and further purified by washing with ethanol three times. For comparation, PdRh NPs were also prepared using the same process except that the pH is 3.0. The Pd NBs were also prepared using the same process while using K_2PdCl_4 as metal precursor.

Electrochemical Measurements

All electrochemical experiments were performed using a CHI 600 D electrochemical analyser at 30 ±1 ^{o}C. A standard three-electrode system was used for all electrochemical experiments, which consisted of a platinum wire as the auxiliary electrode, a saturated calomel reference electrode (SCE) and a catalyst modified glassy carbon electrode as the working electrode.

Potentials in this study were reported with respect to the SCE. The catalyst ink was prepared by ultrasonic the mixture of 10 mg catalyst and 5 mL H_2O for 30 min, and 6 μL of the resulting suspension was drop-cast onto the surface of the glassy carbon electrode. After drying at room temperature, 3 μL of nafion solution (5 wt. %) was covered on the modified electrode surface and allowed drying again. Thus, the working electrode was obtained, and the specific loading of metal on the electrode surface was about 170 μg cm^{-2}. Electrochemical measurements were conducted in N_2-saturated 1 M KOH solution or N_2-saturated 1 M KOH solution with 1 M CH_3CH_2OH. The electrochemically active surface areas (ECSA) of catalysts was calculated from the following equation (ECSA=Q/mC, m was the loading amount of Pd metal) by integrating the reduction charge (Q) of surface $Pd(OH)_2$ and assuming a value of 420 μC cm^{-2} (C) for the reduction charge of a $Pd(OH)_2$ monolayer on the Pd surface, because ECSA of Pd catalysts could not be precisely assessed by coulometry in the "hydrogen region" due to the interference of hydrogen absorption in bulk Pd.

Characterization

X-ray diffraction (XRD) patterns were obtained with a Model D/max-rC X-ray diffractometer using Cu Ka radiation source (λ=1.5406 Å) and operating at 40 kV and 100 mA. X-ray photoelectron spectroscopy (XPS) measurements were carried out on a Thermo VG Scientific ESCALAB 250 spectrometer. The binding energy was calibrated by means of the C 1s peak energy of 284.6 eV. Transmission electron microscopy (TEM) images were taken using a JEOL JEM-2100F transmission electron microscopy operated at 200 kV. High-resolution TEM (HRTEM) and Scanning TEM (STEM) measurements were performed on FEI Tecnai G2 F20 microscope equipped with an EDAX X-ray detector.

Part II: Figures and Tables

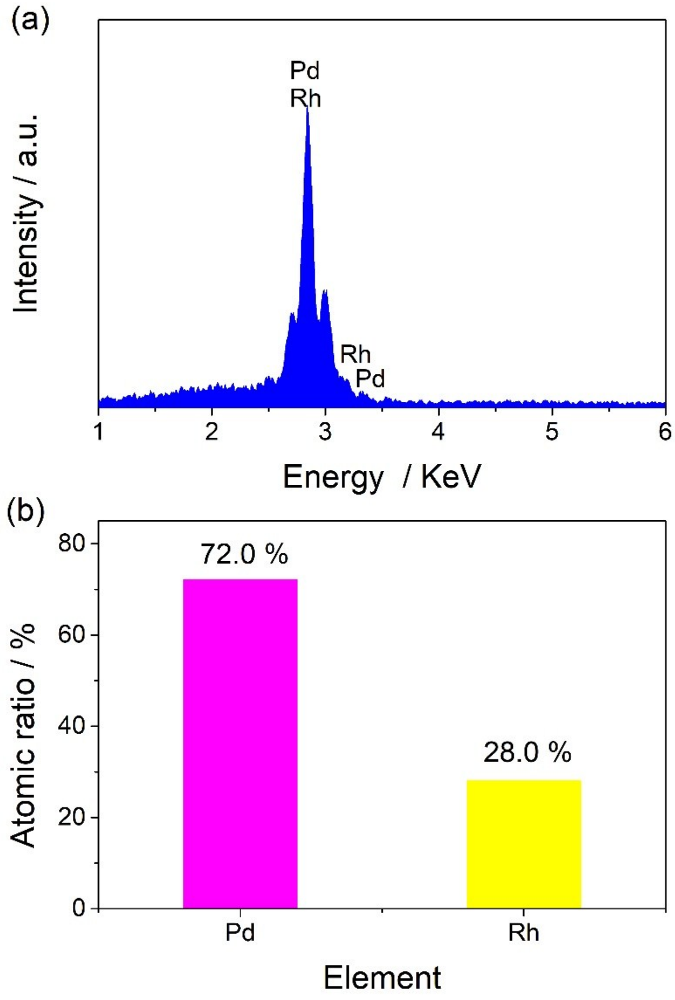

Fig. S1 EDX spectrum of (a) PdRh nanobowls and (b) the corresponding atomic ratio of Pd and Rh.

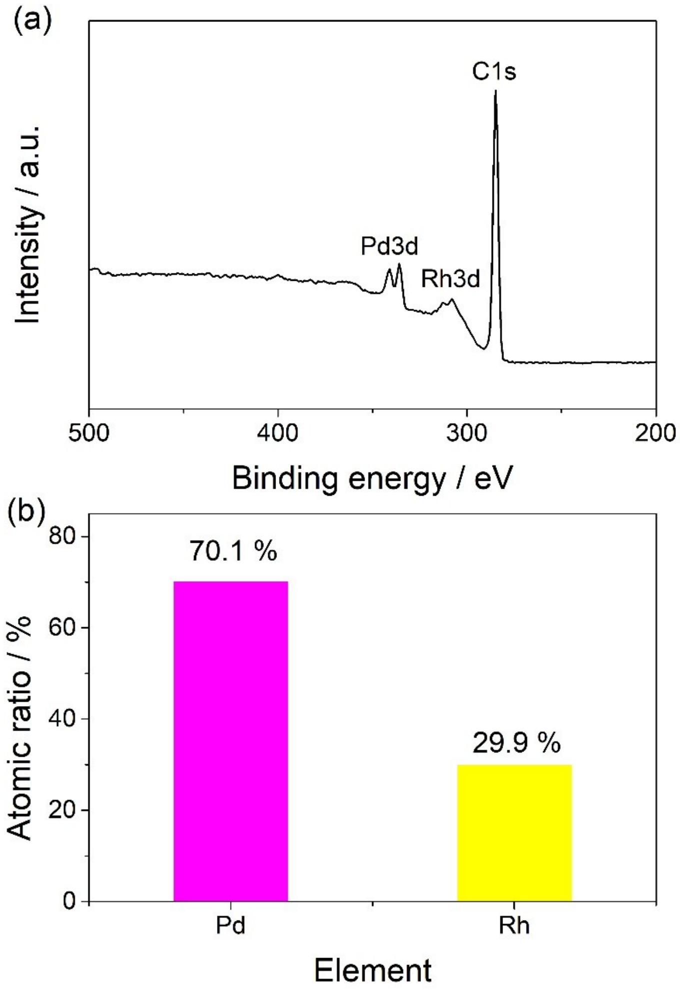

Fig. S2 Full XPS spectrum of (a) PdRh nanobowls and (b) the corresponding atomic ratio of Pd and Rh.

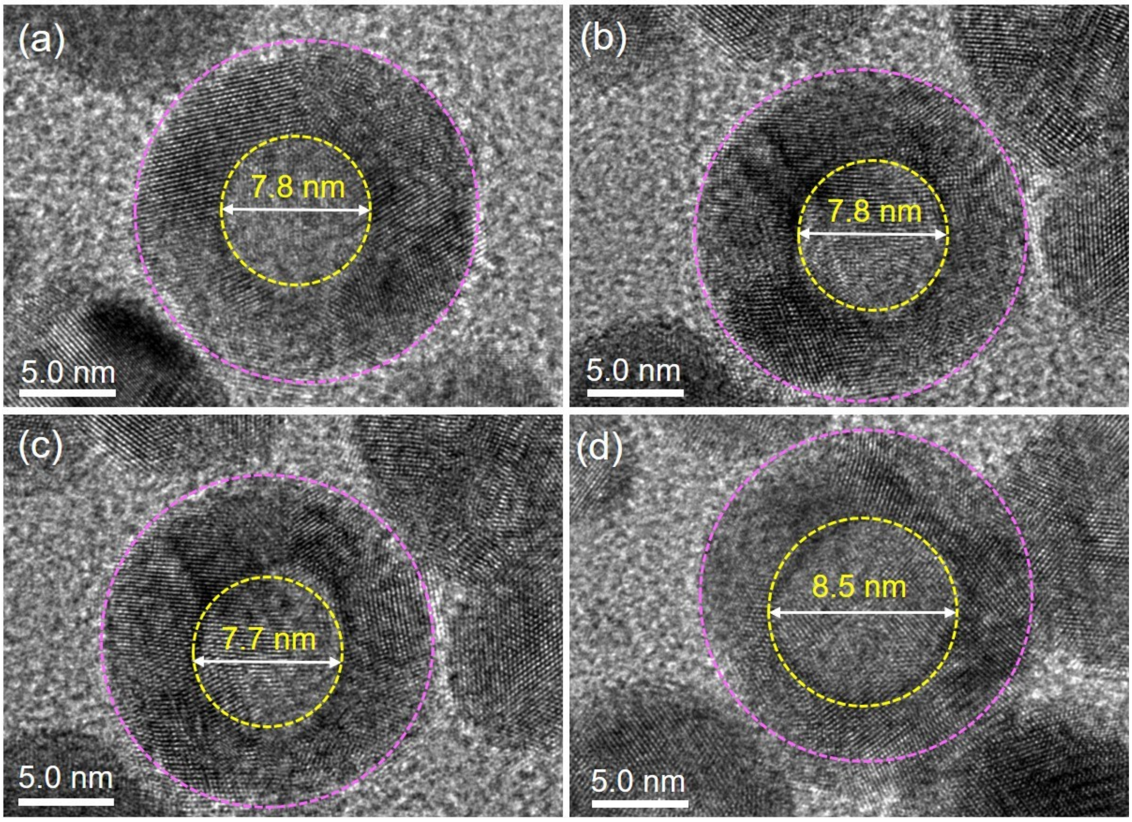

Fig. S3 TEM images of different PdRh nanobowls. The width of hollow center is calculated to be about 7.95 nm.

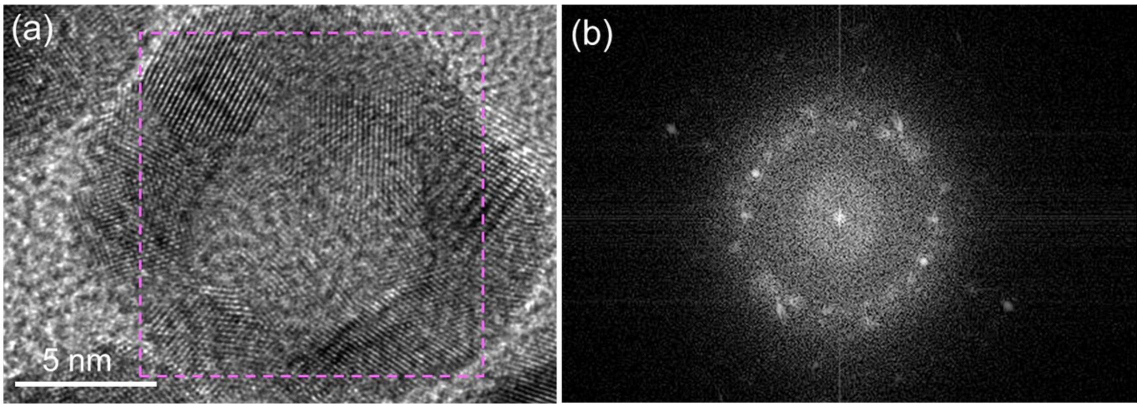

Fig. S4 (b) HRTEM image of an individual PdRh NBs; (b) The corresponding FFT pattern of the HRTEM image.

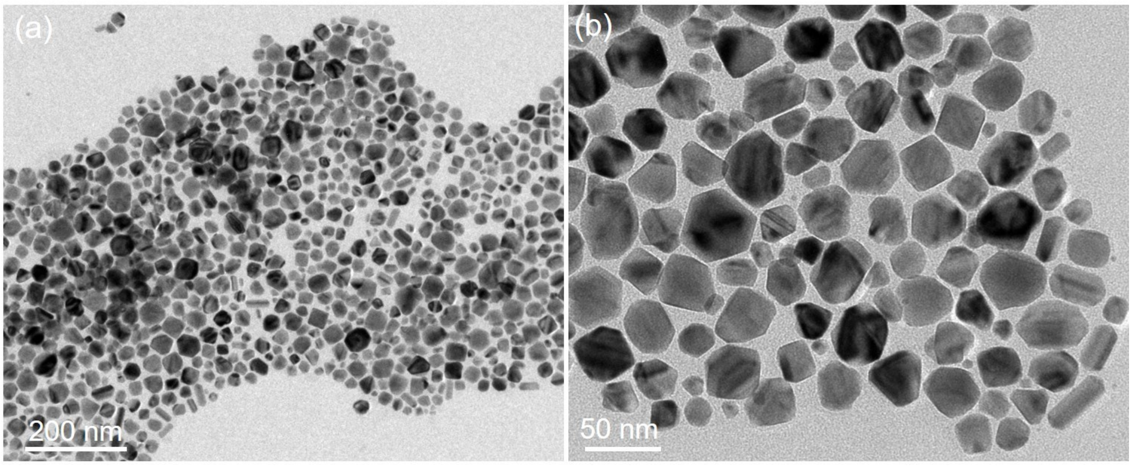

Fig. S5 TEM images of PdRh NPs prepared using the standard procedure except for the absence of urea.

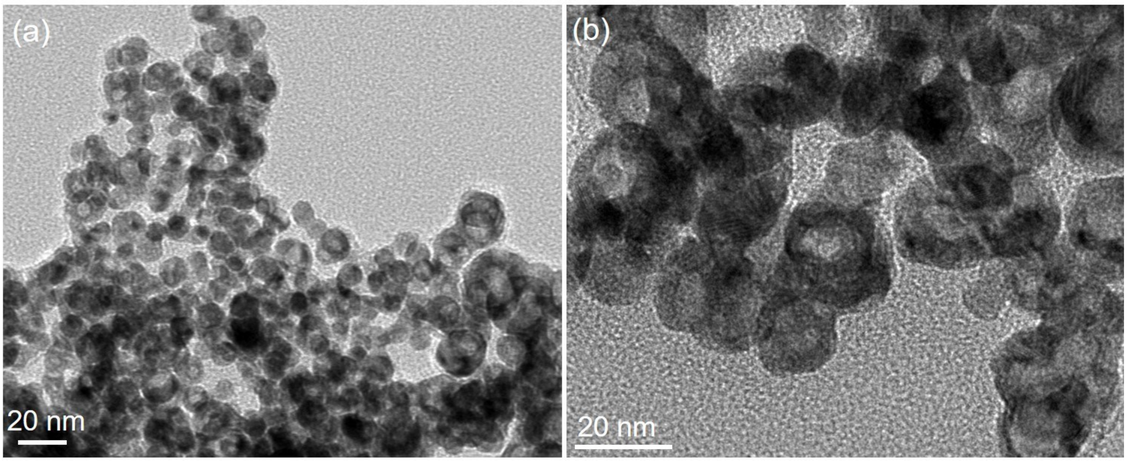

Fig. S6 (a-b) TEM images of PdRh nanocrystals prepared using the standard procedure except for the absence of PVP.

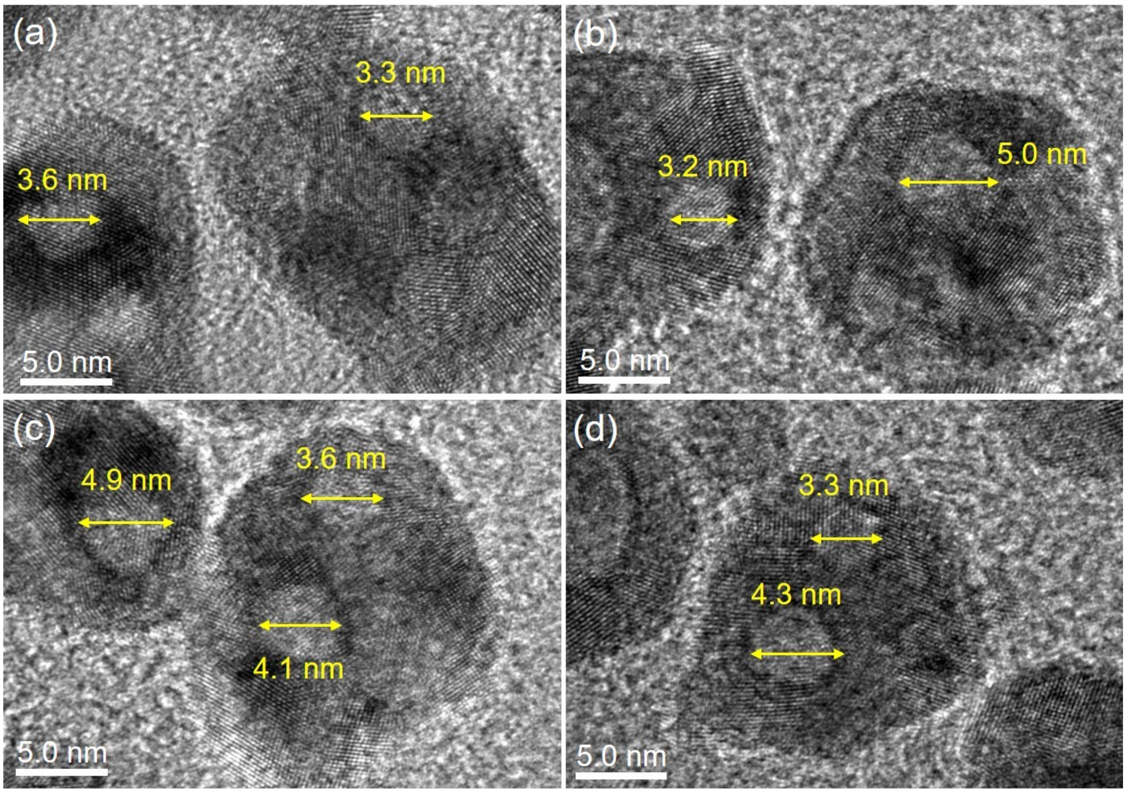

Fig. S7 TEM images of different PdRh nanocages. The width of pore is calculated to be about 3.92 nm.

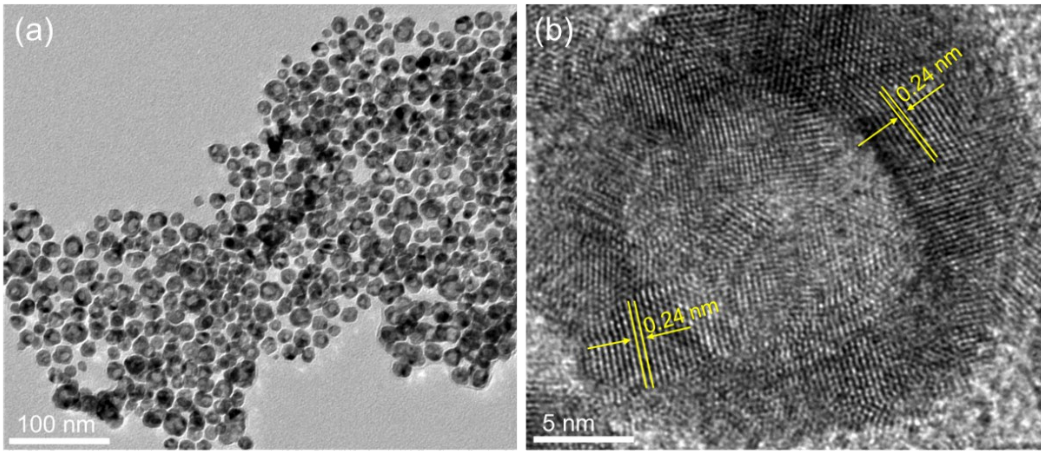

Fig. S8 TEM images of Pd NBs at different magnification.

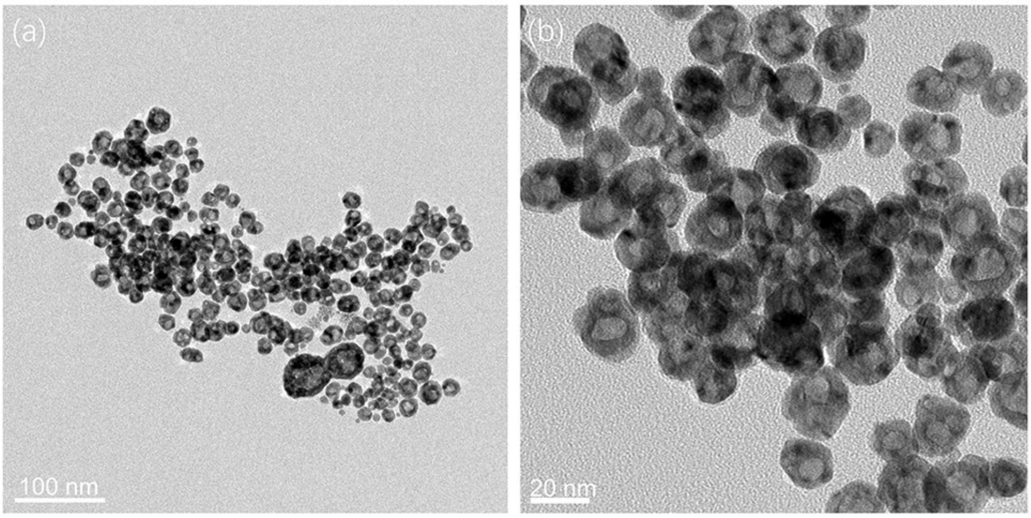

Fig. S9 TEM images of the recovered catalyst.

Table S1. Activity comparisons of PdRh NBs with the previous reported catalysts for the EOR.

Catalyst	Mass activity (mA mg $^{-1}$)	Specific activity (mA cm $^{-2}$)	Electrolyte solution	Ref
PdRh NBs	682	4.8	1 M KOH + 1 M CH_3CH_2OH	this work
Pd NBs	386.7	3.6	1 M KOH + 1 M CH_3CH_2OH	this work
Pd black	172.8	1.7	1 M KOH + 1 M CH_3CH_2OH	this work
Ni@PdAg nanowires	622	0.97	1 M KOH + 0.5 M CH_3CH_2OH	1
Pd–PEDOT/GE	458.5	3.3	1 M KOH + 1 M CH_3CH_2OH	2
PdAg/CNT	305	~	1 M KOH + 1 M CH_3CH_2OH	3
Pd/PANI/Pd SNTAs	~50	~	1 M KOH + 1 M CH_3CH_2OH	4
$Pd_{33}Ag_{67}$	570	2.45	1 M KOH + 1 M CH_3CH_2OH	5
Pd/B-N-doped graphene	464.5	~	1 M KOH + 1 M CH_3CH_2OH	6
Pd/TiO_2	33.06	1.25	1 M KOH + 0.1 M CH_3CH_2OH	7
Au@Pd CNBs	222	~	1 M KOH + 0.5 M CH_3CH_2OH	8
Pd_3Ru_1	613	~	1 M KOH + 1 M CH_3CH_2OH	9
Pd/carbon fiber cloth	495.8	1.84	1 M KOH + 1 M CH_3CH_2OH	10
Pd nanowire arrays	291.7	~	1 M KOH + 1 M CH_3CH_2OH	11
PdRh/C	~	about 0.5	1 M KOH + 1 M CH_3CH_2OH	12
50% Rh/Pd(poly)	~	6.5	0.1 M KOH + 0.4 M CH_3CH_2OH	13

Part III: References

1. F. Guo, Y. Li, B. Fan, Y. Liu, L. Lu and Y. Lei, *ACS Appl. Mater. Interfaces*, 2018, 10, 4705–4714.
2. R. Yue, H. Wang, D. Bin, J. Xu, Y. Du, W. Lu and J. Guo, *J. Mater. Chem. A*, 2015, **3**, 1077-1088.
3. J. Qi, N. Benipal, C. Liang and W. Li, *Appl. Catal. B: Environ.*, 2016, **199**, 494-503.
4. A. L. Wang, H. Xu, J. X. Feng, L. X. Ding, Y. X. Tong and G. R. Li, *J. Am. Chem. Soc.*, 2013, **135**, 10703-10709.
5. S. Fu, C. Zhu, D. Du and Y. Lin, *ACS Appl. Mater. Interfaces*, 2015, **7**, 13842-13848.
6. Y. Jin, D. Han, W. Jia, G. Huang, F. Li, X. Chen, R. Li, M. Zheng and W. Gao, *J. Electrochem. Soc.*, 2017, **164**, F638-F644.
7. B. Lu, B. Yao, G. Roseman, C. P. Deming, J. E. Lu, G. L. Millhauser, Y. Li and S. Chen, *ChemElectroChem*, 2017, **4**, 2211-2217.
8. J. Zhang, K. Sasaki, E. Sutter and R. Adzic, *Science*, 2007, **315**, 220-222.
9. K. Zhang, D. Bin, B. Yang, C. Wang, F. Ren and Y. Du, *Nanoscale*, 2015, **7**, 12445-12451.
10. S.-H. Ye, J.-X. Feng and G.-R. Li, *ACS Catal.*, 2016, **6**, 7962-7969.
11. C. W. Xu, H. Wang, P. K. Shen and S. P. Jiang, *Adv. Mater.*, 2007, **19**, 4256-4259.
12. E. H. Fontes, C. E. D. Ramos, J. Nandenha, R. M. Piasentin, A. O. Neto and R. Landers, *Int. J. Hydrogen Energy*, 2019, **44**, 937-951.
13. A. Maksić, M. Smiljanić, Š. Miljanić, Z. Rakočević and S. Štrbac, *Electrochim. Acta*, 2016, **209**, 323-331.